



Algorithm for spectrum hole identification in cognitive radio network based on discrete wavelet packet transform enhanced with Hilbert transform

P.Y. Dibal^{a,*}, E.N. Onwuka^a, J. Agajo^b, C.O. Alenoghena^a

^a Telecommunications Engineering Department, Federal University of Technology, Minna, Nigeria

^b Computer Engineering Department, Federal University of Technology, Minna, Nigeria

ARTICLE INFO

Keywords:

Discrete wavelet packet transform
Cognitive radio
Heisenberg uncertainty
Spectrum hole
Threshold

ABSTRACT

As wireless devices and applications increase, it is envisioned that spectrum utilization by licensed users will go from low to medium occupancy state. The CRs will need to sense wider bands to obtain free channels. Therefore development of enhanced wideband sensing algorithms is needed. Enhancing old tools for new applications could be quite useful. The discrete wavelet packet transform (DWPT) is a good mathematical tool that can be enhanced for better application in wireless communications. This paper presents an algorithm to identify spectrum holes in a cognitive radio system. The algorithm is based on the application of discrete wavelet packet transform enhanced with Hilbert transform in spectrum sensing. The enhancement with Hilbert transform has the effect of sharpening the PSD edges for better detection. Using histogram analysis for a discrete wavelet packet decomposed signal, the algorithm which we call DWPT-HiSHIA (Discrete Wavelet Packet Transform – Histogram Spectrum Hole Identification Algorithm) determines if a sub-band channel has a spectrum hole or not. Simulation results show the effectiveness of the algorithm in the identification of spectrum holes in sub-band channels for a discrete wavelet packet decomposed signal.

1. Introduction

In today's world, wireless devices and services have become an integral part of human life. Thus, these devices and services can be said to have a pervasive influence on modern human societies. The resultant effect of this is the exponential growth in the number of wireless devices, services, and applications [1,37,38,42], all of which have increased the problem of spectrum scarcity in the available electromagnetic radio spectrum. A second contributing factor to the scarcity of spectrum is the lack of dynamism in the way and manner regulatory agencies allocate spectrum to primary users. This has resulted in a less than optimal utilization of the spectrum because investigation as shown in Fig. 1 [2] has indicated that most primary users hardly make complete utilization of their allocated spectrum at a given temporal and spatial locations.

To mitigate the effect of these two causative factors of spectrum scarcity, cognitive radio technology has been proposed in literature. It is a smart wireless communication system capable of acquiring spectral information from its surrounding environment by operating autonomously. Through this autonomous operation, a cognitive radio is able to evaluate its spectral environment, and then dynamically access suitable spectrum. The autonomy is driven by suitable algorithms embedded at

the heart of the cognitive operations, which confers intelligence on the device. All of these means that the performance of a CR largely depends on the algorithm driving it. In literature, there are two broad categories of spectrum sensing: narrowband and wideband sensing [55]. In narrowband sensing algorithms, the CR senses one channel at a time, but in wideband sensing, a CR can search for spectrum holes across a stretch of channels. It is foreseen that in the near future, spectrum occupancy will attain a medium level, and CRs will have to search further to find a usable vacant spectrum. In such scenario, wideband sensing will become very necessary. Therefore, in this work an algorithm for spectrum hole identification in a wideband spectrum using DWPT is presented.

2. Algorithms in cognitive radio technology

A cognitive radio (CR) is a smart wireless communication system which operates by dynamically accessing radio spectrum not occupied by the licensed primary users of such spectrum. To achieve the desired smartness, algorithms play a central role in all areas of a cognitive radio cycle. The cognitive radio cycle as depicted in Fig. 2 [3], is characterized by four major components which include spectrum sensing, spectrum mobility, spectrum decision, and spectrum sharing.

From Fig. 2, spectrum sensing is arguably the most important

* Corresponding author.

E-mail address: yoksa77@gmail.com (P.Y. Dibal).

PLM, Amateur, Others: 30 - 54 MHz	
TV 26, nc: 54.00 MHz	
Air Traffic Control, Aero nav: 108 - 138 MHz	
Fixed Mobile, Amateur, Others: 138 - 174 MHz	
TV 7 - 13: 174 - 216 MHz	
Maritime Mobile, Amateur, Others: 216 - 225 MHz	
Fixed Mobile, Aero, Others: 225 - 406 MHz	
Amateur, Fixed Mobile, Radiolocation: 406 - 470 MHz	
TV 14 - 20: 470 - 512 MHz	
TV 21 - 36: 512 - 608 MHz	
TV 37 - 51: 608 - 698 MHz	
TV 52 - 69: 698 - 806 MHz	
Cellphone and SMP: 806 - 902 MHz	
Unlicensed: 902 - 928 MHz	
Paging, SMS, Fixed, Rx, AUX, and FMS: 928 - 960 MHz	
IFF, TACA, GPS, Others: 960 - 1240 MHz	
Amateur: 1240 - 1300 MHz	
Aero Radar, Military: 1300 - 1400 MHz	
Space, Fixed Mobile, Telemetry: 1400 - 1525 MHz	

Fig. 1. Fixed spectrum allocation.

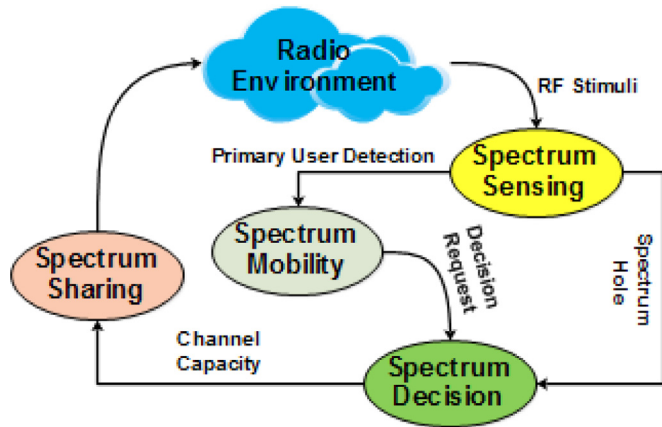


Fig. 2. Cognitive cycle of cognitive radio.

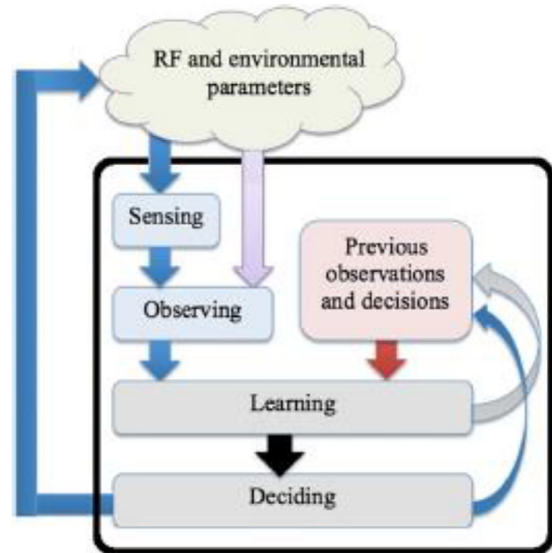


Fig. 3. Tasks performed by algorithms in a cognitive radio cycle.

spectrum management function performed by a CR because it is fundamental to any other operation carried out by that CR. Spectrum sensing involves continuous monitoring of the radio frequency (RF) environment with speed and accuracy in order to identify and make available unutilized frequency band for use by the CR [3,4]. Spectrum mobility is an operation which ensures that there is no interruption in communication whenever the CR makes a transition to a better spectrum [5]. On the other hand, spectrum decision is an operation which decides how long unlicensed or secondary users can use unutilized frequency bands. This is achieved by selecting an operating channel for the secondary user (SU); the channel selected must be detected as vacant through spectrum sensing [6,7]. The fourth component of the cognitive radio cycle is spectrum sharing. This operation ensures that unutilized frequency bands in a frequency spectrum are fairly distributed for use among unlicensed users without harmful interference to other users [8–10].

From the description of the components of the CR cycle, it can be seen that CR is a complex technology which relies heavily on algorithms to perform the complicated tasks required to make it a viable technology. Hence, the algorithms must be robust and reliable in order to achieve the desired level of functionality which includes dynamic adaption of transmission waveform, selection of optimum channel access method, spectrum use, and networking protocols [24]. These functionalities guarantee that the CR will achieve good network

performance and resource management. Fig. 3 [25] depicts the tasks performed by algorithms in the CR cycle.

In the sensing and observation stage, the algorithms sense the radio environment for parameters such as the characteristics of channels between base stations and users, the power available in a spectrum, the availability of spectrum holes in the time frequency domain (which is the focus of this paper), and local policies [25,26]. At the learning stage, the algorithms take the previous observations and decisions on one hand, and the current observations on the other hand as inputs, with the sole aim of minimizing power consumption, bit error rate, interference, maximizing spectrum efficiency, quality of service, and throughput [27,28]. The algorithms at the decision stage make decision on frequency band allocation, allocation of time slot, coding and adaptive modulation, antenna selection parameters, and routing plan [29,30].

3. Spectrum hole in spectrum sensing

A spectrum hole by definition is a band of frequencies allocated to a

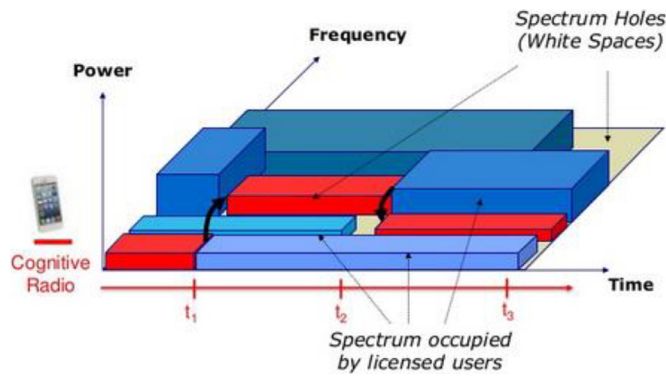


Fig. 4. Spectrum band with spectrum holes or white spaces.

licensed user, but at a particular instance of the space-time continuum, such band is unutilized by the licensed primary user [11], thereby making such a spectrum to lie momentarily idle or empty. Fig. 4 [12] depicts a spectrum band with spectrum holes or white spaces in it.

A spectrum hole can be viewed from the time domain, and the frequency domain. In the time domain, a spectrum hole is the interval in time in which a primary user is not transmitting. In the frequency domain, a spectrum hole is a frequency band that a secondary user can use in transmission without causing interference to all primary users across all frequencies. In terms of classification, there are basically two types of spectrum holes – temporal spectrum holes and spatial spectrum holes [13,14]. A temporal spectrum hole occurs when a primary user is not transmitting during the time of sensing, hence a secondary user can utilize the spectrum hole at that slot of time. Spatial spectrum hole on the other hand occurs when a frequency band is unutilized by primary users in some spatial areas even though such a band may be in use in another area, thereby giving secondary users in the area the opportunity to occupy such bands. Different techniques could be used to efficiently identify spectrum holes in a given spectrum. One such technique, used in wideband spectrum sensing, is the Discrete Wavelet Packet Transform (DWPT).

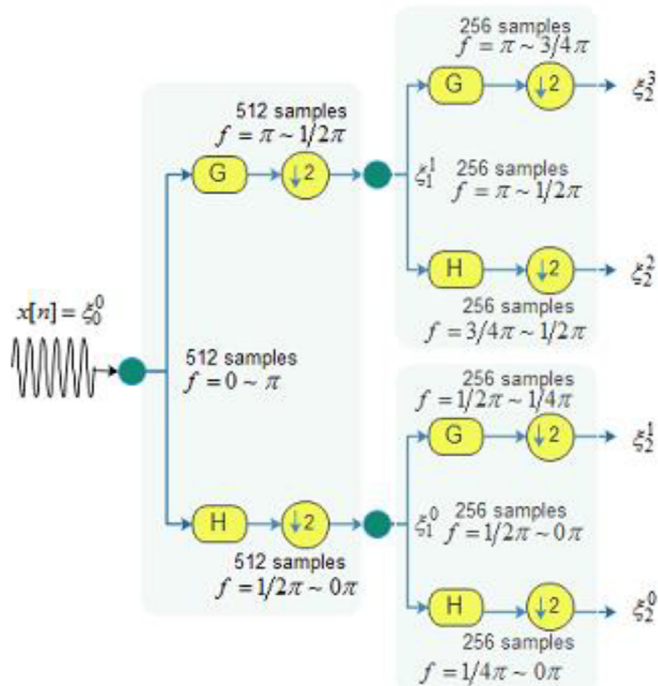


Fig. 5. Analysis filter bank of a wavelet packet.

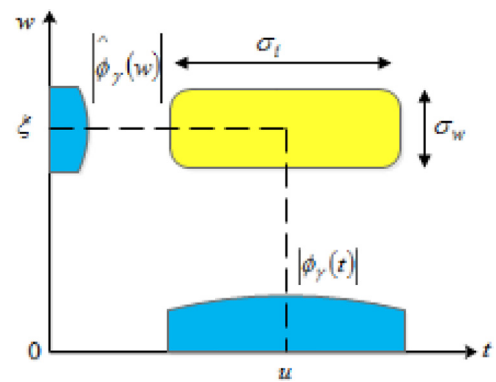


Fig. 6. Heisenberg box representing an atom ϕ_γ .

4. Discrete wavelet packet transform

Wavelets are extensively applied in the analysis of data, they are powerful mathematical tools that are used in the representation of both known and unknown signals as a set of functions with the sole aim of gaining better insight into their characteristics. Wavelets operate by decomposing an input signal into different frequency components, which are then studied with resolutions that match their time-scales. The discrete wavelet packet transform as shown in Fig. 5 [16] is a generalization of wavelet transform in which a tree structure is used in the implementation of the wavelet algorithm by decomposing an input signal through high-pass and low-pass filter branches [15,17–19].

Wavelet packet transforms produce waveforms which are called atoms and are indexed by position, scale, and frequency [20]. The decomposition of an input signal by a wavelet packet, recursively splits each parent node into two subspaces $W_{n,j}$ which are orthogonal and located according to Ruch and Patrick [21] at:

$$W_{n,j} = W_{2n,j-1} \oplus W_{2n+1,j-1} \quad (1)$$

where n is a nonnegative integer, j is the decomposition level, and \oplus is

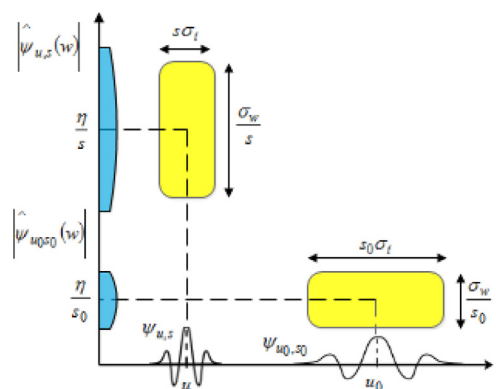


Fig. 7. Heisenberg time-frequency boxes of two wavelets $\psi_{u,s}$ and ψ_{u_0,s_0} .

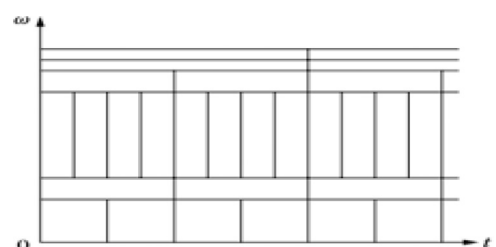


Fig. 8. Heisenberg boxes covering each frequency interval of the wavelet packet.

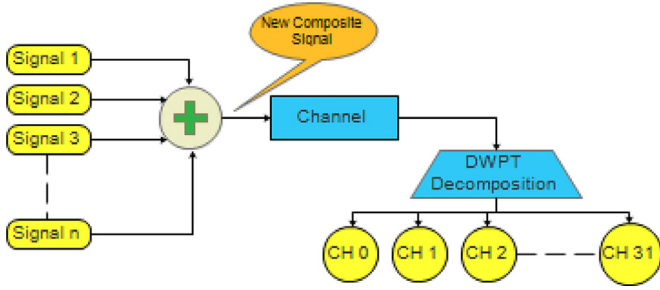


Fig. 9. Cognitive radio receiver model for application of the DWPT algorithm.



Fig. 10. A 22 × 32 matrix generated from terminal nodes of wavelet packet tree.

orthogonal addition.

For the wavelet packet tree shown in Fig. 5, the wavelet packet coefficients $\xi_{l+1}^{2p}[n]$ are generated using the scaling filter. Similarly, the coefficients $\xi_{l+1}^{2p+1}[n]$ are generated using the wavelet filter. Mathematically, the coefficients are expressed as [16]:

$$\xi_{l+1}^{2p}[n] = \sqrt{2} \sum_k h[k] \xi_l^p[2n - k], n = 0, 1, \dots, N - 1 \quad (2)$$

$$\xi_{l+1}^{2p+1}[n] = \sqrt{2} \sum_k g[k] \xi_l^p[2n - k], n = 0, 1, 2, \dots, N - 1 \quad (3)$$

where $h[k]$ is the low-pass filter, $g[k]$ is the high-pass filter, and p is the position at level l .

For the signal in each sub-band channel, the energy is calculated as

Table 1
Input signal parameters.

	Amplitude	Frequency (MHz)
Signal 1	1.3	15
Signal 2	1.7	40
Signal 3	2.0	67
Signal 4	1.8	81

[22,23]:

$$E = \frac{1}{T} \int_0^T \left[\sum_{j \geq j_0} \sum_k c_{j,k} \phi_{j,k}(t) + d_{j,k} \psi_{j,k} \right]^2 dt \quad (4)$$

$$E = \frac{1}{T} \sum_{j \geq j_0} \sum_k (c_{j,k}^2 + d_{j,k}^2) \quad (5)$$

where $c_{j,k}$ is scaling function coefficient, $d_{j,k}$ is the wavelet function coefficient. It should be noted that the presence of a signal in a sub-band channel makes the energy level of that signal in the sub-band channel higher. Also, the position of the signal in the sub-band channel can be resolved in terms of both time and frequency using time-frequency analysis of the signal with well-known techniques like the Heisenberg boxes [34]. For the wavelet transformer shown in Fig. 5, the output was enhanced with the Hilbert transform in order to make the sub-band frequency edges sharper and easier to detect [36].

Edge detection enhancement using Hilbert transform is novel ideal which is possible because the spread of the instantaneous frequency derived from the Hilbert transform of a signal is always less than the bandwidth of the signal. As a result of this, the detection of edges of frequencies in a wideband signal as depicted in Fig. 5 can be better and sharper with Hilbert transform. We refer to our work in [36] for more

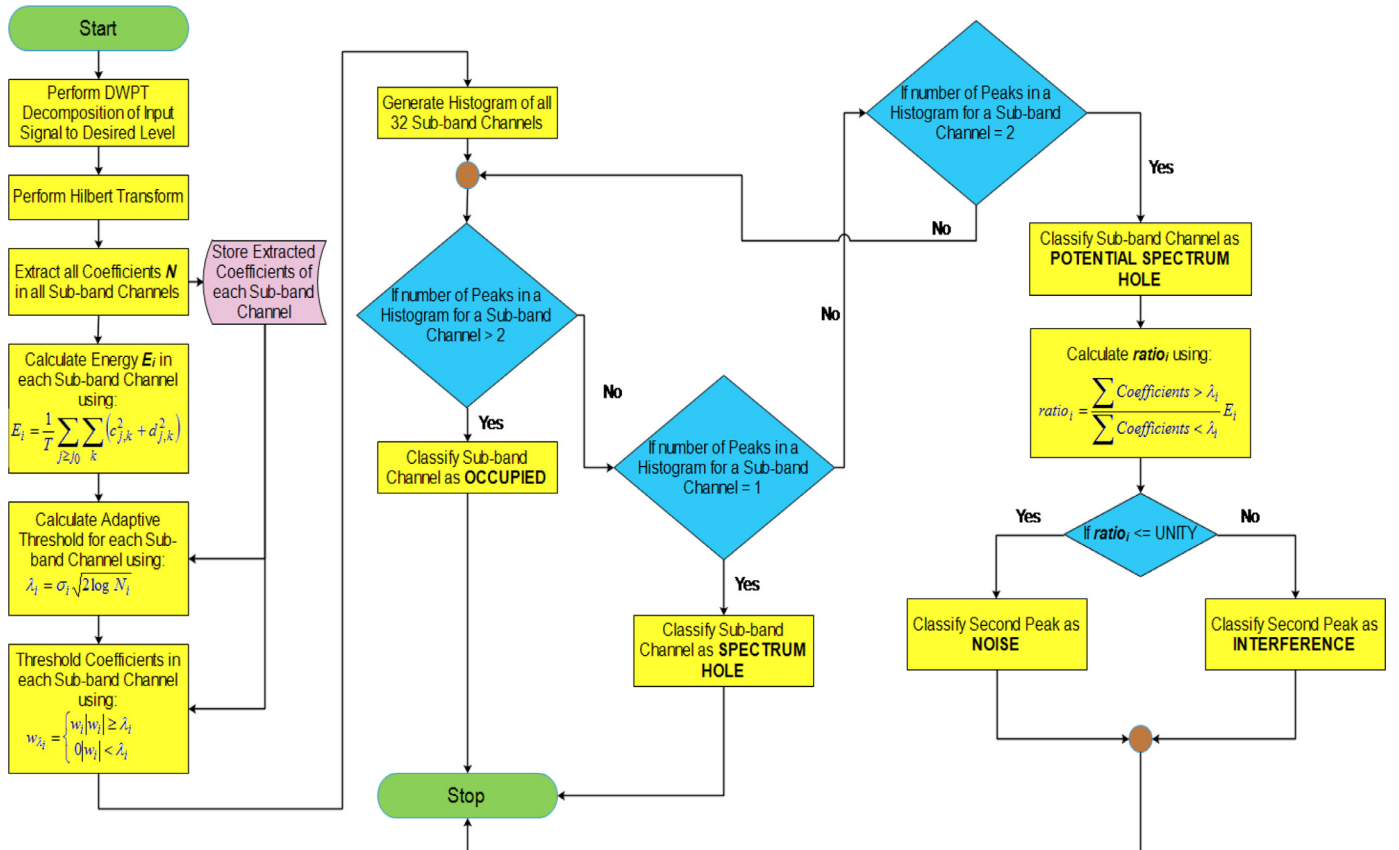


Fig. 11. Flow chart of algorithm to identify spectrum holes in sub-band channels.

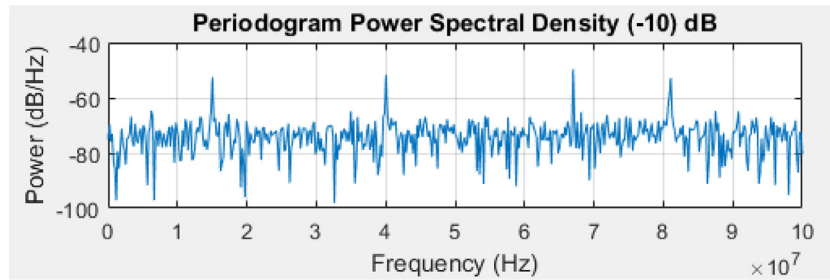


Fig. 12. Input power spectrum density at -10 dB.

details on this.

5. Time–frequency analysis of a wavelet packet using Heisenberg uncertainty

Given a time-frequency dictionary $D = \{\varphi_\gamma\}_{\gamma \in \Gamma}$ composed of waveforms of unit norm $\|\varphi_\gamma\| = 1$, the localization u of ϕ_γ and the spread of ϕ_γ around u is defined in [34,35] as:

$$u = \int t |\varphi_\gamma(t)|^2 dt \quad \text{and} \quad \sigma_{t,\gamma}^2 = \int |t - u|^2 |\varphi_\gamma(t)|^2 dt \tag{6}$$

The frequency localization ξ of $\hat{\varphi}_\gamma$ and the spread of $\hat{\varphi}_\gamma$ around ξ given as:

$$\xi = (2\pi)^{-1} \int w |\hat{\varphi}(w)|^2 dw \quad \text{and} \quad \sigma_{w,\gamma}^2 = (2\pi)^{-1} \int |w - \xi|^2 |\hat{\varphi}(w)|^2 dw \tag{7}$$

Taking (6) and (7) into consideration, the Fourier Parseval re-

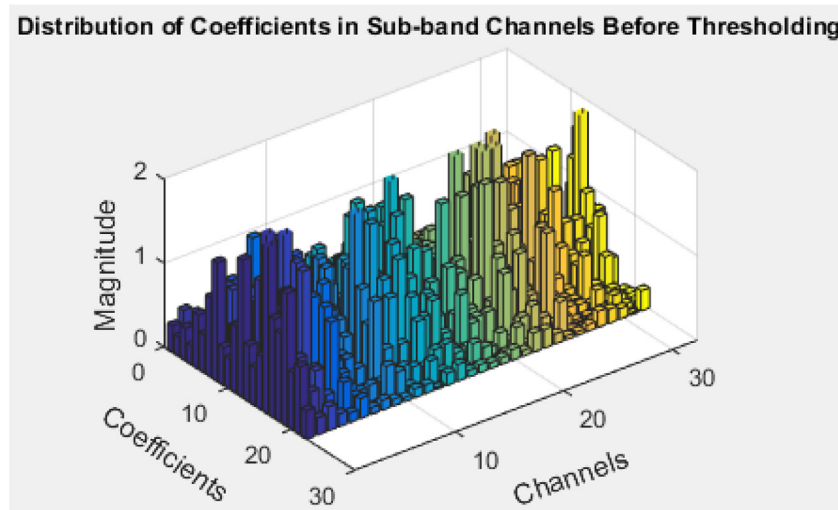


Fig. 13. Distribution of sub-band channel coefficients after Hilbert transformation at -10 dB.

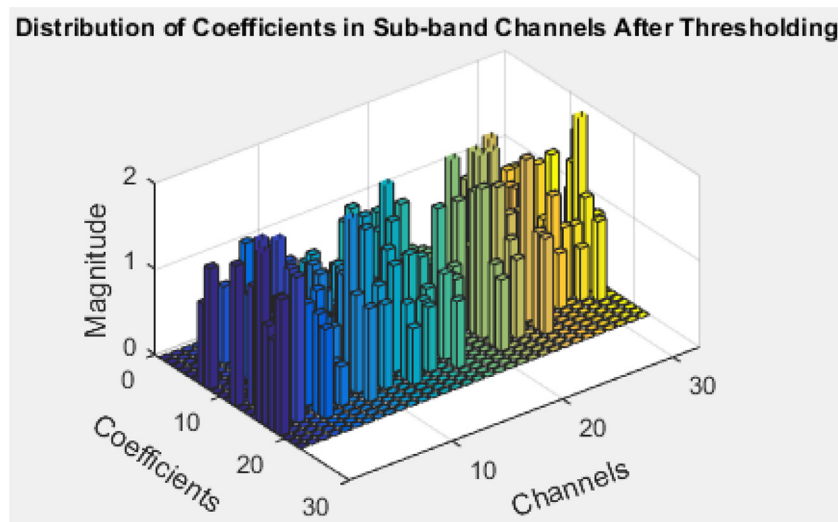


Fig. 14. Distribution of sub-band channel coefficients after thresholding at -10 dB.

Table 2
Algorithm results for spectrum hole identification at SNR of -10 dB.

Channel	Noise	Interference	Channel	Noise	Interference
0	0	0	16	0	0
1	0	0	17	0	1
2	0	0	18	1	0
3	0	0	19	1	0
4	0	1	20	0	1
5	0	0	21	0	1
6	0	0	22	0	0
7	1	0	23	0	0
8	0	0	24	0	1
9	0	1	25	1	0
10	0	0	26	1	0
11	0	0	27	1	0
12	0	0	28	0	0
13	1	0	29	0	0
14	0	0	30	0	0
15	0	0	31	0	0

relationship states that:

$$\langle f, \varphi_\gamma \rangle = \int_{-\infty}^{+\infty} f(t)\varphi_\gamma^*(t)dt = \frac{1}{2\pi} \int_{-\infty}^{+\infty} \hat{f}(w)\hat{\varphi}_\gamma(w)dw \quad (8)$$

The relationship in (8) implies that $\langle f, \varphi_\gamma \rangle$ depends mostly on the values of $f(t)$ and $\hat{f}(w)$, where $\varphi_\gamma(t)$ and $\hat{\varphi}_\gamma(w)$ are non-negligible in a rectangle centered at (u, ξ) of size $\sigma_t, \sigma_w, \gamma$. The rectangle is shown in Fig. 6. The rectangular box also called a Heisenberg box or time-frequency atom, is a quantum of information over a resolution cell. Hence, the construction of a dictionary of time-frequency atoms can be viewed as the coverage of the time-frequency plane with resolution cells having a time width σ_t, γ and frequency width σ_w, γ .

If we define s as a scale, u as a position, and η as the center of a positive frequency interval, then for a wavelet atom $\psi_{u,s}$ its Heisenberg box is a rectangle centered at $(u, \eta/s)$, having time and frequency widths proportional to s and $1/s$. A variation in s will cause a change in the

time-frequency resolution cell, with the area remaining constant. This concept is illustrated in Fig. 7.

In wavelet packets, the Heisenberg boxes cover each frequency interval of the wavelet packet functions, which are translated in time so as to cover the whole plane. Fig. 8 illustrates this concept. The tiling in Fig. 8 is obtained by translating in time the wavelet packets covering each frequency interval.

6. Spectrum hole identification algorithm

To identify the holes in a signal decomposed using discrete wavelet packet transform (DWPT), the DWPT-HiSHIA algorithm is developed in such a way that certain operations are performed on the coefficients of each sub-band channel in order to determine the presence or otherwise of spectrum holes in that sub-band channel. To determine the presence of the spectrum holes, we propose two hypotheses H_0 which indicates the signal below a threshold i.e. noise, when the primary user is absent, and H_1 which indicates the signal above threshold when the primary user is present [39]:

$$H_0: x(n) = w(n) \quad (9)$$

$$H_1: x(n) = s(n) + w(n) \quad (10)$$

In (9), $w(n)$ indicates the presence of white Gaussian noise with zero mean and variance σ_w^2 ; also, the primary user is absent in (9) as made by the observation $x(n)$. In (10), the observation $x(n)$ is such that the primary user is present, $s(n)$, alongside the presence of noise $w(n)$. From (9) and (10), the probability that an SU accurately declares the presence of a primary user (PU) when the spectrum is actually occupied is the probability of detection (P_d); the probability that an SU declares the presence of a PU when the spectrum is actually idle is the probability of false alarm (P_f); the probability that an SU declares the absence of a PU when the spectrum is actually occupied is the probability of miss-detection (P_m). Mathematically, P_d, P_f, P_m are expressed as follows [40,41]:

$$P_d = \Pr(H_1|H_1) = \Pr(E > \lambda|H_1) \quad (11)$$

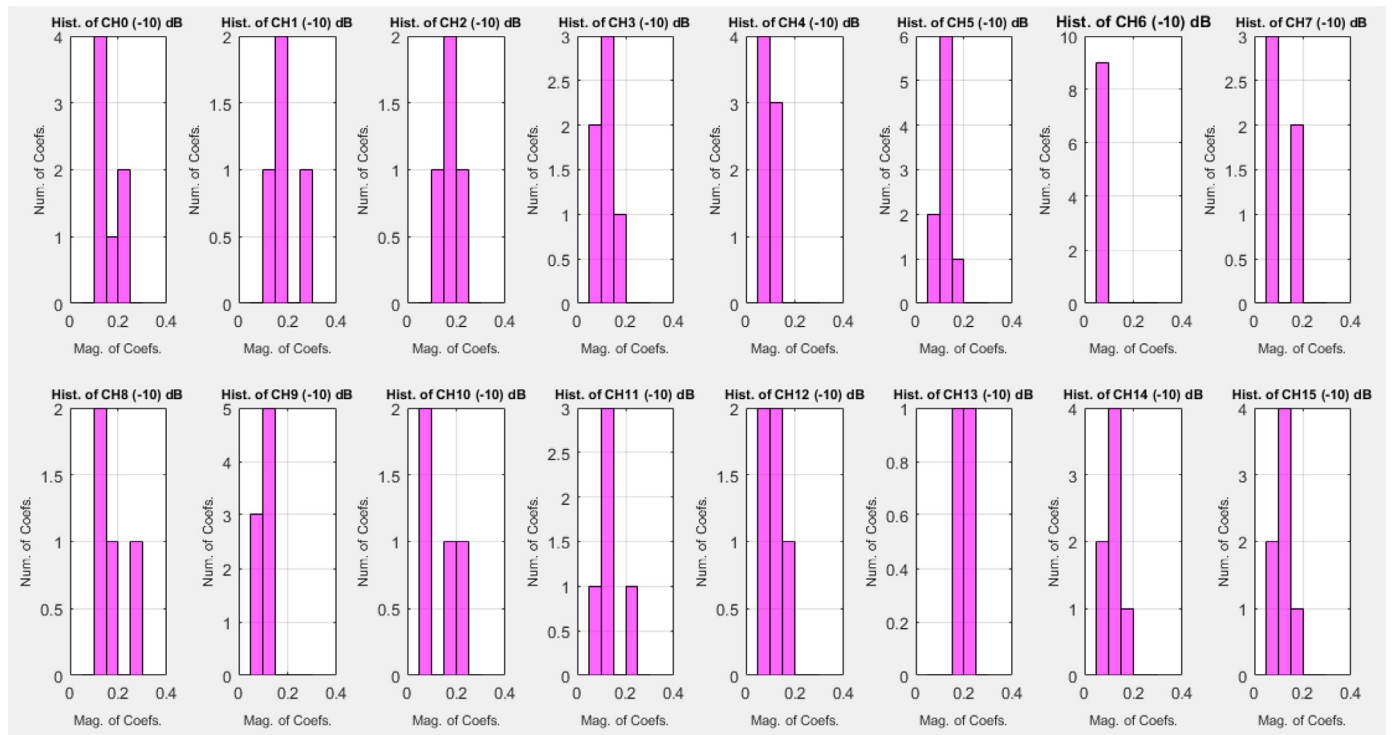


Fig. 15. Histogram for channels 0 to 15 at -10 dB.

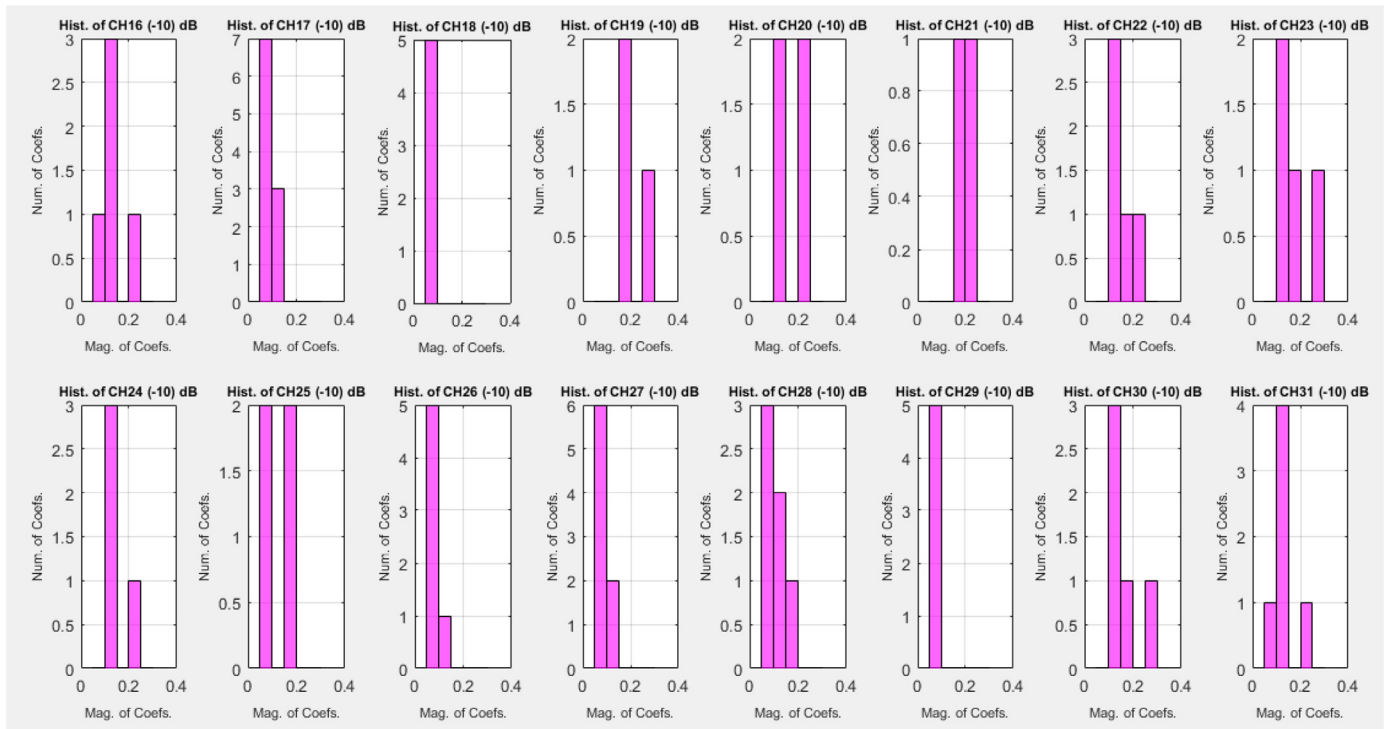


Fig. 16. Histogram for channels 16 to 31 at -10 dB.

Table 3
Status of sub-band channels after application of algorithm at -10 dB.

Occupied channels	Channel with complete spectrum hole	Channels having spectrum hole with noise	Channels having spectrum hole with interference
0, 1, 2, 3, 5, 8, 10, 11, 12, 14, 15, 16, 22, 23, 28, 30, 31	6, 29	7, 13, 18, 19, 25, 26, 27	4, 9, 17, 20, 21, 24

$$P_f = \Pr(H_1|H_0) = \Pr(E > \lambda|H_0) \tag{12}$$

$$P_m = \Pr(H_0|H_1) = \Pr(E < \lambda|H_1) \tag{13}$$

where E is the received energy in the DWPT sub-band channel defined by (5), and λ is the applied threshold.

Fig. 9 shows the model of the CR receiver system in which the DWPT-HiSHIA algorithm will be applied.

The incoming signal(s) to the channel could be one or more signal(s) of different frequencies, but whose frequency lies within the band of interest. These signal(s) are added together to create a composite signal

that contains all the incoming signals which are clearly identifiable by their location in frequency (see Fig. 12). If a spectrum hole is identified in any of the sub-band channels after the DWPT decomposition, it implies that for the entire frequency band of the composite signal entering the channel, there are some frequencies that are vacant. The DWPT-HiSHIA algorithm then generates the DWPT coefficients and use them to identify these vacant frequencies in the composite signal coming from the channel.

At 5 levels of decomposition, the DWPT will have 32 channels each having 22 coefficients. This is shown in Fig. 10.

In the DWPT-HiSHIA algorithm, $w(n)$ defined in (9) and (10) is identified as either noise or interference. It is noise if the observation is less than or equal to the given threshold of UNITY. It is interference if it is greater than the given threshold of UNITY. The algorithm is defined as follows:

Discrete Wavelet Packet Transform – Histogram Spectrum Hole Identification Algorithm

1. Perform a discrete wavelet packet transform decomposition of the input signal to the desired level.

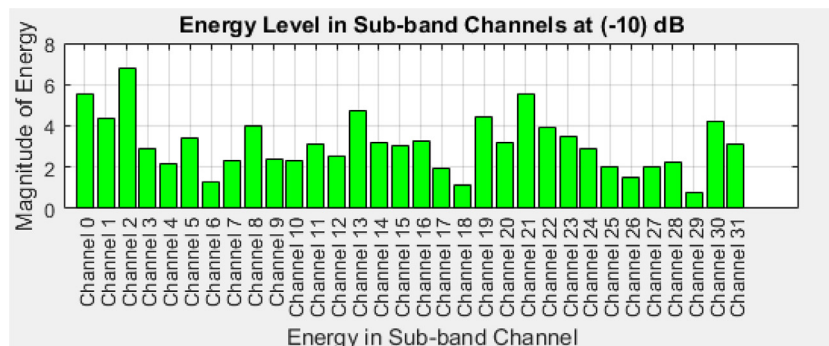


Fig. 17. Energy level in sub-band channels at -10 dB.

Table 4
Results for DWPT-HiSHIA algorithm at SNR of 10 dB.

Channel	Noise	Interference	Channel	Noise	Interference
0	0	0	16	0	0
1	0	0	17	0	1
2	0	0	18	0	0
3	1	0	19	0	0
4	0	1	20	1	0
5	0	0	21	0	0
6	0	0	22	0	1
7	1	0	23	0	0
8	0	0	24	0	1
9	0	1	25	1	0
10	1	0	26	1	0
11	0	0	27	0	1
12	0	1	28	1	0
13	0	0	29	0	0
14	0	0	30	0	0
15	0	0	31	0	0

Table 5
Performance of DWPT-HiSHIA algorithm with increase in SNR from –10 dB to 10 dB.

Performance at –10 dB	Performance at 10 dB
Channel 3 classified as occupied	Channel 3 more accurately classified as spectrum hole with noise
Channel 10 occupied as occupied	Channel 10 more accurately classified as spectrum hole with noise
Channel 12 occupied as occupied	Channel 12 more accurately classified as spectrum hole with interference
Channel 18 classified as spectrum hole with interference	Channel 18 classified more accurately as noise
Channel 20 classified as spectrum hole with interference	Channel 20 classified more accurately as spectrum hole with noise

2. Take the Hilbert transform of the discrete wavelet packet decomposed signal.
3. Perform a channel-by-channel extraction of all the coefficients in the sub-band channels of the wavelet packet tree.
4. Calculate the energy E_i in each sub-band channels of the wavelet packet tree.
5. Generate an adaptive threshold for each sub-band channel by using the Donoho-Johnstone relationship [31]: $\lambda_i = \sigma_i \sqrt{2 \log N_i}$ (14)
6. Threshold the coefficients in channel i against the computed

$$\text{threshold } \lambda_i \text{ using: } w_{\lambda_i} = \begin{cases} w_i & |w_i| \geq \lambda_i \\ 0 & |w_i| < \lambda_i \end{cases} \quad (15)$$

where w_i is the wavelet packet coefficient in channel i before thresholding, w_{λ_i} is the wavelet packet coefficient in channel after thresholding.

7. Generate histogram for all the 32 sub-band channels.
8. If the number of peaks in a histogram for a sub-band channel is more than two, classify the sub-band channel as OCCUPIED. This is because the peaks indicate that the coefficients in that sub-band channel are well distributed across the frequency there; hence the presence of a primary user signal.
9. If the number of peaks in a histogram for a sub-band channel is one, classify the sub-band channel as a SPECTRUM HOLE. This is because the single peak indicates that all coefficients in that sub-band channel are approximately equal to the value of zero; hence the lack of spread of the coefficients in the sub-band channel.
10. If the number of peaks in a histogram for a sub-band channel is two, take the ratio of the number of coefficients greater than the threshold λ_i for that channel to the number of coefficients less than the threshold λ_i for that channel, and multiply by the energy E_i of than channel i.e. $ratio_i = \frac{\text{Coefficients} > \lambda_i * E_i}{\text{Coefficients} < \lambda_i}$ (16)
11. If $ratio_i \leq UNITY$ classify the second peak as noise.
12. If $ratio_i > UNITY$ classify the second peak as interference.

The flow chart representation of the DWPT-HiSHIA algorithm is shown in Fig. 11. It should be noted that the threshold is chosen according to the nature of the input signal, signal-to-noise ratio, and channel coefficients.

7. Performance evaluation

To evaluate the performance of the algorithm developed in Section 6, we perform a number of simulations, and then analyze the results obtained. The simulation is performed using MATLAB, along with its digital signal processing and wavelet toolboxes. The experiment involves a composite signal having different amplitudes and frequencies as described in Table 1. The power spectral density (PSD) of the input signal at SNR of –10 dB is shown in Fig. 12. The distribution of the coefficients for the PSD which is obtained after decomposition of the input signal by the wavelet packet decomposition function into sub-band channels, i.e., after the Hilbert transformation and before thresholding, is shown in Fig. 13.

Fig. 14 shows the effect of the adaptive thresholding on the distribution of the coefficients in each sub-band channel.

The performance of the algorithm is tested and the results obtained are shown in Table 2.

The generated histogram by the algorithm for all the 32 channels are shown in Figs. 15 and 16.

It can be seen from Table 2 and Figs. 15 and 16 that the DWPT-HiSHIA algorithm identified the channels that are occupied as those having more than two peaks in the histogram and also having noise and interference values of 0. The DWPT-HiSHIA algorithm also identified channels with complete spectrum holes as channels 6 and 29 in Figs. 15

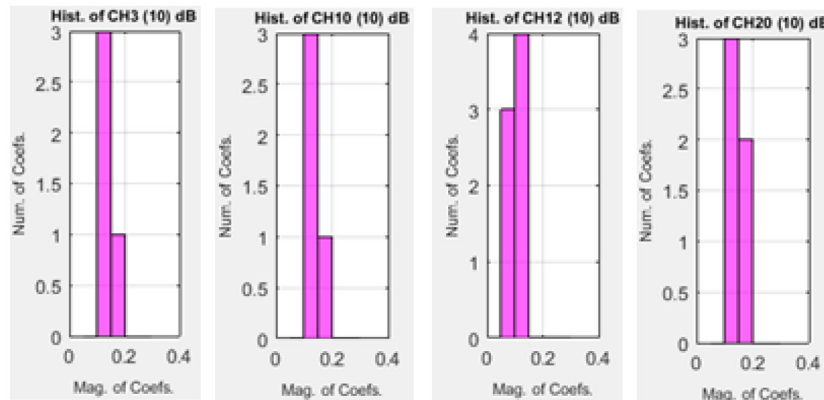


Fig. 18. Classification of sub-band channels 3, 10, 12, and 20 at 10 dB.

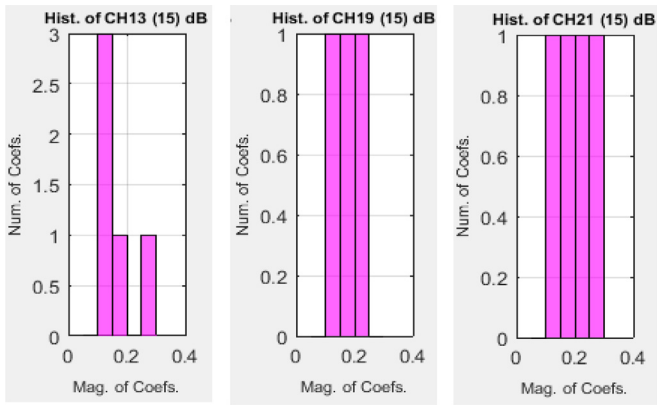


Fig. 19. Classification of sub-band channels 13, 19, and 21 at 15 dB.

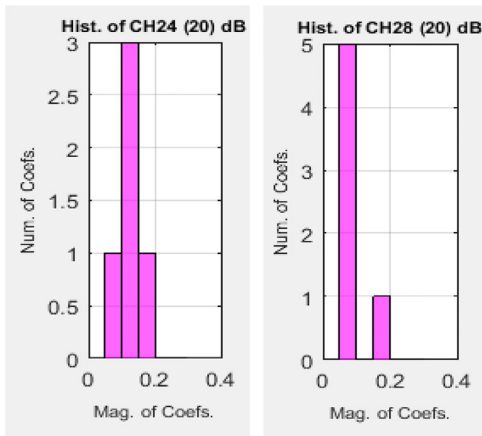


Fig. 20. Classification of sub-band channels 24, and 28 at 20 dB.

and 16, having only one peak with noise and interference values of 0. This identification was made possible because these channels contain noise signals whose coefficients are approximately zero thereby indicating the presence of noise and hence a spectrum hole. Using the same pattern, the DWPT-HiSHIA algorithm identified spectrum holes with noise, and spectrum holes with interference from channels with only two peaks. Table 3 is derived from a combination of Table 2 and Figs. 15 and 16.

The estimations and identification made by the algorithm is further corroborated by the energy level in each channel as shown in Fig. 17.

To verify the performance of the algorithm, the simulation is repeated again by setting the signal-to-noise ratio (SNR) to 10 dB. At this SNR value, the performance of the DWPT-HiSHIA algorithm is tested and the results obtained are shown in Table 4.

Table 5 summarizes the comparison made between the performance of the DWPT-HiSHIA algorithm at -10 dB and 10 dB from Table 2 and Table 4.

The state of channels 3, 10, 12, and 20 at 10 dB are shown in Fig. 18.

A comparison between Tables 2, 4, and 5 shows that there was a case of false alarm in channels 3, 10, 12, 20, at -10 dB. The false alarm occurred at -10 dB because at low SNR value, the noise competes with the signal in strength; hence, a detection technique can easily classify a noisy channel as OCCUPIED (which is a false alarm). However, as the SNR value increases, the signal strength increases, thus making a detection technique more accurate in detection and classification of sub-band channels.

The performance of the DWPT-HiSHIA algorithm was tested at 15 dB, and sub-band channels 13, 19, and 21 in Fig. 19 are shown to be occupied.

A comparison between the state of sub-band channels 13, 19, 21 in Figs. 15, 16 and 19 shows a case of missed-detection in these sub-band channels at -10 dB. This is because the sub-band channels were classified as UNOCCUPIED channels at -10 dB, whereas they are actually OCCUPIED as shown in Fig. 19.

At 20 dB the DWPT-HiSHIA algorithm classified sub-band channel

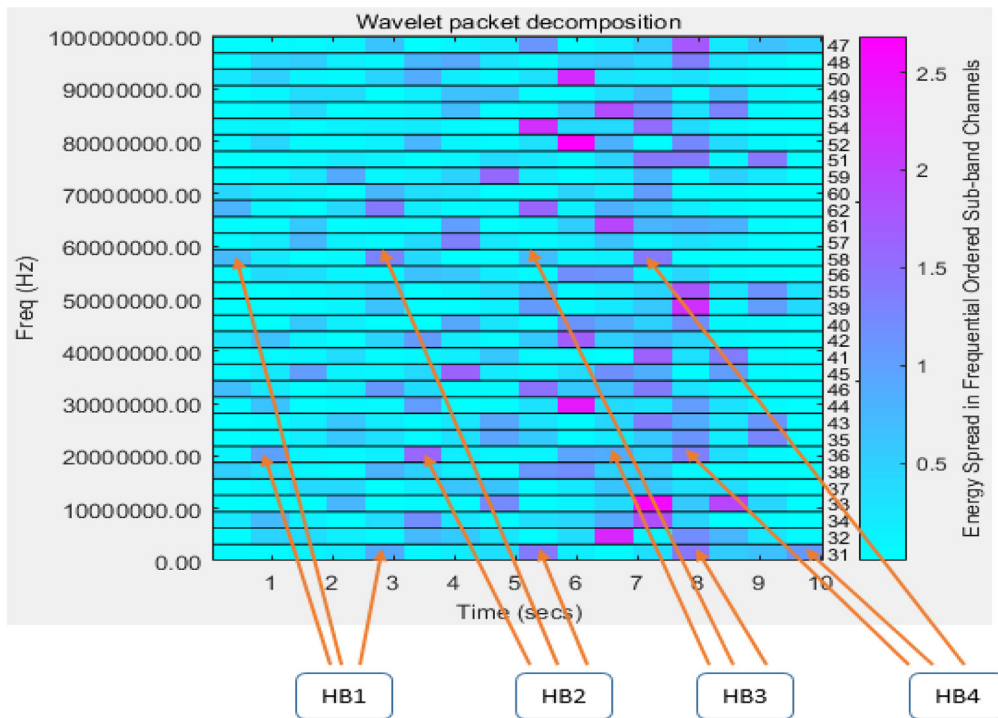


Fig. 21. Time-frequency representation of decomposed signal using Heisenberg boxes.

24 as OCCUPIED channel as shown in Fig. 20. A comparison with the state of this sub-band channel at -10 dB reveals a case of missed-detection owing to the fact that it was declared as UNOCCUPIED channel at -10 dB, when it is actually an OCCUPIED channel. Also, the DWPT-HiSHIA algorithm classified sub-band channel 28 as UNOCCUPIED channel at 20 dB in Fig. 20. A comparison with the state of this sub-band channel at -10 dB in Fig. 16 shows a case of false alarm in the channel at -10 dB.

8. Time–frequency analysis of decomposed signal using Heisenberg boxes

Using the Heisenberg boxes in Section 5, the time-frequency representation of the decomposed signal which covers each frequency interval of the wavelet packet is shown in Fig. 21. In this Fig, the left y-axis is the wide-band frequency of entire input spectrum, the right y-axis is the sequential order of the 32 sub-band channels of the DWPT. For all the 32 sub-band channels, it can be seen that there are four Heisenberg boxes in each channel; this is exactly the number of input single tone signals in the wide-band spectrum as shown in Fig. 12. Also, the distance between the Heisenberg boxes (as shown by HB1 to HB4) in Fig. 21 matches the distance between the single tone signals in Fig. 12. This confirms that the vacant frequencies between the single tone signals in the wide-band input signal remain vacant after decomposition.

It should also be noted that all the 32 sub-band channels have four Heisenberg boxes of varying intensity, which correspond to the energy levels. This is because for a DWPT, the energy in the input signal is distributed across sub-bands due to shifts in the input signal [32,33]. In sub-band channels which are classified as spectrum holes, having low intensity, the energy from the input signal is approximately zero.

9. Comparison with other DWPT spectrum sensing techniques

The DWPT-HiSHIA algorithm competes favorably with other DWPT spectrum sensing techniques in literature which are summarized in Table 6. It has low complexity like the techniques in row 1 and 3 in Table 6 because it is also based on energy detection. However it outperforms the technique in row 1 in speed because it uses logical deduction based on the spread of coefficients to make its classification of sub-band channels. The use of the Hilbert transform in the DWPT-HiSHIA algorithm makes it have better sub-band frequency edge detection [36], hence it has better accuracy at low SNR than the technique in row 3. The DWPT-HiSHIA algorithm has better data throughput than the technique in row 2 because it does not need to scan a wide range of spectrum continuously. In terms of accuracy, the technique in row 4 outperforms the DWPT-HiSHIA algorithm because it is based on Cyclostationary feature detection. However, the DWPT-HiSHIA algorithm outperforms it in terms of speed since energy detection requires less sensing time than Cyclostationary feature detection. The DWPT-HiSHIA algorithm outperforms the technique in row 5 in terms of speed since it uses logical deduction for its classification instead of double thresholding. At high degrees of decomposition, the use of MAC in the technique in row 6 will make it slower than the DWPT-HiSHIA algorithm.

10. Comparison with other spectrum sensing techniques

The performance of the DWPT-HiSHIA algorithm is also compared with other spectrum sensing techniques and presented in Table 7. It can be seen that owing to the fact that the algorithm is based on the DWPT and Hilbert transform, it competes favorably with most of the spectrum sensing techniques for all the performance metrics considered.

From Tables 6 and 7, it is clear that the novelty and contribution of the DWPT-HiSHIA algorithm when compared to other DWPT spectrum sensing techniques on one hand, and other spectrum sensing techniques on the other hand is in terms of speed, complexity, and accuracy.

Table 6
DWPT spectrum sensing techniques in literature.

S/N	Author(s)	Year	Title of Paper	Metrics	Strength	Weakness
1	Kang, A. S., Sharma, V., & Singh, J. S.	(2017)	Efficient Spectrum Sensing using Discrete Wavelet Packet Transform Energy in Cognitive Radio.	Measured the power in sub-band channels using wptdec function.	It has low complexity because the technique is based on energy detection	The use of MAC for second stage sensing makes the technique undesirable when a high degree of decomposition is involved and at the same time meeting a tight constraint of speed.
2	Aswathy, D., & Sruthi, S.	(2014)	Discrete Wavelet Packet Transform Based Cooperative Spectrum Sensing for Cognitive Radios.	Measured probability of detection against probability of false alarm.	Cooperative spectrum sensing provides better performance than single user based spectrum sensing.	It has a low data throughput because it has to scan a wide range of spectrum.
3	Shrutika, S., & Kumbhar, M. S.	(2012)	Performance of Wavelet Packet Based Energy Detector for Spectrum Sensing.	Measured probability of detection against signal to noise ratio.	It has low complexity because the technique is based on energy detection.	Low frequency selectivity between transition bands. It has poor accuracy at low SNR.
4	Bakhit, A. A., & Alfateh, M., & Varun, J.	(2010)	Discrete Wavelet Packet Transform Based Multiresolution Spectrum Sensing using Cyclostationary Feature Detector.	Measured probability of detection against SNR.	The combination of DWPT and Cyclostationary feature detection gives the technique good accuracy at low SNR.	The use of Cyclostationary feature detection implies the technique will require a long observation time in order to achieve spectrum sensing.
5	Sunghyun, K., Youngwoo, Y., Hyungsuk, J., Minjae, K., & Hyuckjae, L.	(2008)	Selective Discrete Wavelet Packet Transform Based Energy Detector for Cognitive Radios.	Measured detection probability against received mean power of primary user. Also measured missed detection probability against received mean power of primary users.	The use of elliptic IIR filters gave better roll-off characteristics than Butterworth IIR filters in the implementation of DWPT.	The use of double thresholding increases the sensing time of the technique.
6	Youngwoo, Y., Hyungsuk, J., Holyoon, J., & Hyuckjae, L.	(2007)	Discrete Wavelet Packet Based Energy Detector for Cognitive Radios.	Measured the power in each sub-band channel.	The DWPT used in spectrum sensing has lower complexity owing to its implementation with IIR polyphase filters.	The use of MAC for second stage sensing makes the technique undesirable when a high degree of decomposition is involved and at the same time meeting a tight constraint on speed.

Table 7
Comparison of proposed algorithm with other spectrum sensing techniques.

	DWPT-HISHIA algorithm	Cyclostationary detection	Matched filter	Continuous wavelet	Waveform based detection	Eigenvalue based detection
Speed	Has high speed because the addition of the Hilbert transform does not add any significant latency as no domain transformation is required [43–44]. Leverages on the time- frequency resolution capability of DWPT (enhanced with Hilbert transform for sharper edges) to yield high accuracy [36,50].	Requires long observation before making a decision [45]. Performs well at low signal-to-noise ratio [45].	Has high latency due to the amount of time required to obtain perfect knowledge of PU signal [46]. Accuracy depends on perfect knowledge of PU signal, which is not practical in all cases [46].	Difficult to use in real-time because it is computationally intensive [47]. Not very accurate when minimum latency must be maintained [47].	The requirement of knowledge of PU user signal implies the speed of this technique may be undesirable when high sensing speed is required [48]. Accuracy depends on the quality of preamble patterns used for synchronization; this can be a challenge at low SNR [48].	Requires long sensing time to compute eigenvalues when rank of signal matrix representation is large [49]. It outperforms proposed algorithm because it is insensitive to noise uncertainty [49].
Accuracy	Requires no prior information of the PU signal [43,44,50].	Requires prior information of the type of carrier, and cyclic prefixes [51].	Requires prior information of PU signal like modulation technique and spreading codes [52].	Requires no prior information of the PU signal [47,50].	Requires preamble patterns for synchronization purposes [53].	Requires no prior information of PU signal [54].
Preprocessing signal information	The complexity is low because the technique only makes decisions on the magnitude of each coefficient in a sub-band channel [43,44].	Requires very high complexity in computation [45].	Requires very high complexity in computation [52].	Has very high complexity which always introduces excessive redundancy in a design [47].	Has low complexity in implementation [49].	The complexity depends on the rank of the matrix used in representing the signal [49].

11. Conclusion

In this paper, we presented an algorithm for the identification of spectrum holes in wideband spectrum in a cognitive radio network based on the Hilbert transform of the discrete wavelet packet transform. It is noted that wideband sensing will become handy in the near future when CRs may need to sense more channels at once to identify usable ones. The algorithm measured the degree of skewness of the coefficients in each channel of the discrete wavelet packet transform decomposed signal. The pattern of the degree of skewness was used to generate a histogram, from which an analysis based on the number of peaks in the histogram was carried out to determine if a spectrum hole is available in the sub-band channel or not. Computer simulations were performed on Matlab to test the algorithm at signal-to-noise ratio values of -10 dB, 10 dB, 20 dB, and 30 dB. The results obtained showed that the algorithm performed well, with increasing accuracy as SNR was increased. The Heisenberg box was also used to display the time-frequency distribution of the signals. Comparisons with other DWPT sensing schemes for CR were made, and the scheme was also compared with general sensing schemes in the CR arena. It is noteworthy that the edge enhancement of the DWPT with Hilbert Transform is a worthwhile improvement as it will enable better detection in lower SNR when compared to similar techniques.

Acknowledgment

We acknowledge the funding support we got from TETFUND with grant number: TETFUND/FUTMINNA/2017/B/04.

References

- [1] Cisco Visual Networking Index: Global mobile data traffic forecast update 2015–2020. Online. Available at: [http://www.cisco.com/c/en/us/solutions/collateral/service-provider/visual-networking-index-vni/mobile-white-paper-c11-520862.html]. Retrieved: 13/01/2017.
- [2] M. Maurad, H. Aziza, Major spectrum sensing techniques for cognitive radio networks. A survey, *Int. J. Eng. Innovative Technol.* 5 (3) (2015) 24–37.
- [3] G. Manikandan, N. Mathavan, M. Suresh, M. Paramasivam, V. Lavanya, Cognitive radio spectrum sensing techniques – a survey, *Int. J. Adv. Eng. Technol.* 3 (2) (2016) 48–52.
- [4] Saloni, P. Batra, Spectrum sensing in cognitive radio by statistical matched wavelet method and matched filter, *Int. J. Electron. Commun. Technol.* 7 (1) (2016) 33–39.
- [5] A. Sharma, M. Katoch, Analysis of various spectrum sensing techniques in cognitive radio, *Int. J. Adv. Res. Comput. Sci. Softw. Eng.* 5 (5) (2015) 1100–1104.
- [6] S. Shelly, M. Sangman, An energy-efficient game-theory-based spectrum decision scheme for cognitive radio sensor networks, *Sensors* 1009 (2016) 1–20.
- [7] D.S. Rao, G. Naidu, P. Prasad, QoS based spectrum selection scheme in cognitive radio networks, *J. Netw. Commun. Emerg. Technol.* 6 (1) (2016) 12–17.
- [8] A. Arunkumar, S. Kumaran, Cooperative relaying spectrum sharing in cognitive radio networks, *Int. J. Appl. Theor. Sci. Technol.* 2 (1) (2016) 1012–1018.
- [9] S. Christani, J.N. Patel, Approaches to spectrum sensing and spectrum sharing algorithms in cognitive radio networks: a survey, *Int. J. Innovative Res. Comput. Commun. Eng.* 4 (2) (2016) 1297–1302.
- [10] M. Ahmed, S. Aduwati, B. Ali, M. Othman, Dynamical spectrum sharing and medium access control for heterogeneous cognitive radio networks, *Int. J. Distrib. Sens. Netw.* 2016 (2016) 1–15.
- [11] S. Haykin, Cognitive radio: brain-empowered wireless communication, *IEEE J. Sel. Areas Commun.* 23 (2) (2005) 201–220.
- [12] N.S. Mohamed, Cognitive radio, *Int. J. Curr. Eng. Technol.* 6 (4) (2016) 1357–1359.
- [13] M. Negi, S. Singh, SVSS: selective variant intelligent spectrum sensing for cognitive radio, *Int. J. Adv. Res. Comput. Commun. Eng.* 5 (7) (2016) 152–157.
- [14] M. Shaika, M. Amin, Cognitive radio technology – a smarter approach, *Int. J. Sci. Eng. Technol. Res.* 5 (2) (2016) 607–612.
- [15] B.V. Mahala, M.J. Anand, Adaptive wavelet packet decomposition for efficient image denoising by using neighsure shrink method, *Int. J. Comput. Sci. Inf. Technol.* 5 (4) (2014) 5003–5009.
- [16] H. Nikookar, Wavelet Radio: Adaptive and Reconfigurable Wireless Systems Based on Wavelets, Cambridge University Press, UK, 2013.
- [17] S. Elango, G. Thirugnanam, P. Mangaiyarkarasi, Wavelet packet based video watermarking and extraction using independent component analysis, *J. Adv. Inf. Technol.* 7 (3) (2016) 156–160.
- [18] B. Ilker, W.S. Ivan, On the dual-tree complex wavelet packet and M-band transforms, *IEEE Trans. Signal Process.* 56 (6) (2008) 2298–2310.
- [19] L. Li, Y. Han, W. Chen, C. Lv, D. Sun, An improved wavelet packet-chaos model for life prediction of space relays based on voltterra series, *PLoS One* 11 (6) (2016) 1–13, <http://dx.doi.org/10.1371/journal.pone.0158435>.

- [20] Mathworks, Wavelet Packets, Online. Available at: <http://www.mathworks.com/help/wavelet/ug/wavelet-packets.html>, (2017) Accessed 15/01/2017.
- [21] D.K. Ruch, J.F. Patrick, *Wavelet Theory: An Elementary Approach with Applications*, Wiley, New Jersey, United States, 2009.
- [22] Q. Zhinjin, N. Wang, G. Yue, C. Laurie, Adaptive threshold for energy detector based on discrete wavelet packet transform, *Wirel. Telecommun. Symp.* (2012) 1–5.
- [23] N. Wei, Z. Chen, A. Zhu, Research on adaptive resolution spectrum sensing method based on discrete wavelet packet transform, *Telkomnika Indonesian J. Electr. Eng.* 12 (2) (2014) 1385–1394.
- [24] S. Peter, S. Douglas, M. Gary, R. Dipankar, Future Directions in Cognitive Radio Research, NSF, 2009 Workshop Report. Online. Available at: https://www.cs.cmu.edu/~prs/NSF_CRN_Report_Final.pdf Accessed 30/01/2017.
- [25] A. Nadine, N. Youssef, A. Karim, Recent advances on artificial intelligence and learning techniques in cognitive radio networks, *EURASIP J. Wirel. Commun. Netw.* 174 (2015) 1–20, <http://dx.doi.org/10.1186/s13638-015-0381-7> 2015.
- [26] O. Goze, M. Cenk, T. Nghi, T. Jian, Energy-efficient power allocation in cognitive radio systems with imperfect spectrum sensing, *IEEE J. Sel. Areas Commun.* 34 (12) (2016) 3466–3481, <http://dx.doi.org/10.1109/JSAC.2016.2621399>.
- [27] K. Snehal, L. Dinesh, Review of decentralized technique in cognitive radio wireless network, *Int. J. Pure Appl. Res. Eng. Technol.* 4 (9) (2016) 106–112.
- [28] J. Gerome, B. Alberto, Spectrum sensing system in software defined radio to determine spectrum availability, *IEIE Trans. Smart Process. Comput.* 5 (2) (2016) 100–106.
- [29] Y. Yuan, B. Paramvir, C. Ranveer, M. Thomas, W. Yunnan, Allocating dynamic time-spectrum blocks in cognitive radio networks, Microsoft Res. (2016) Online. Available at <https://www.microsoft.com/en-us-research/wp-content/uploads/2016/02/bsmart.pdf> Accessed: 01/02/2017.
- [30] S.A. Babatunde, T. Bodhaswar, S. Attahiru, solving resource allocation problems in cognitive radio networks: a survey, *EURASIP J. Wirel. Commun. Netw.* 2016 176 (2016) 1–14, <http://dx.doi.org/10.1186/s13638-016-0673-6>.
- [31] G. Yandong, X. Maojin, Y. Fengyun, M. Yachun, S. Shuang, Improved wavelet threshold De-noising method based on GNSS deformation monitoring data, *J. Eng. Technol. Sci.* 47 (4) (2015) 463–476.
- [32] E.L. Rachel, S.W. Alan, A wavelet packet approach to transient signal classification, *Appl. Comput. Harmon. Anal.* 2 (1995) 265–278.
- [33] G. Matthieu, L. Joel, Performances of complex wavelet packet based multicarrier transmission through double dispersive channel, *IEEE Proceeding of the 7th Nordic Signal Processing Symposium*, 2006, pp. 74–77.
- [34] S. Mallat, *A Wavelet Tour of Signal Processing*. 2nd Ed, Academic Press, New York, 1999.
- [35] C.P. Maria, J. Martin, *Wavelets, their Friends, and what they can do for you*, European Mathematical Society, 2008.
- [36] P.Y. Dibal, E.N. Onwuka, C.O. Alenoghena, J. Agajo, Enhanced discrete wavelet packet sub-band frequency edge detection using Hilbert transform, *Int. J. Wavelets Multiresolution Inf. Process.* 16 (1) (2018) 1850009-1–1850009-17.
- [37] I.F. Akyildiz, L. Won-Yeol, C.V. Mehmet, M. Shantidev, Next generation/dynamic spectrum access/cognitive radio wireless networks: a survey, *Comput. Netw.* 50 (2006) (2006) 2127–2159.
- [38] S. Haykin, Cognitive radio: brain empowered wireless communications, *IEEE J. Sel. Areas Commun.* 23 (2) (2005) 201–220.
- [39] A.J. Onumanyi, E.N. Onwuka, A.M. Aibinu, O.C. Ugweje, M.J.E. Salami, A real valued neural network based autoregressive energy detector for cognitive radio application, *Int. Scholarly Res. Not.* 2014 (2014) 1–11.
- [40] L. Nandita, J. Devendra, Performance of p-norm detector in cognitive radio networks with cooperative sensing in presence of malicious users, *Hindawi Wirel. Commun. Mobile Comput.* (2017), <http://dx.doi.org/10.1155/2017/4316029>.
- [41] E. Waleed, H. Najam, L. Seok, S. Hyung, Intelligent spectrum sensing scheme for cognitive radio networks, *EURASIP J. Wirel. Commun. Netw.* 26 (2013) 1–10 2013.
- [42] A. Onumanyi, E.N. Onwuka, Improved handoff stability using an enhanced vertical handoff decision algorithm, *Sci. Res. Essays* 5 (25) (2010) 4080–4087.
- [43] Y. Younwoo, J. Hyoungsook, J. Hoiyoon, L. Hyuckjae, Discrete wavelet packet based energy detector for cognitive radios, *IEEE Vehicular Technology Conference*, 2007, pp. 2641–2645.
- [44] S. Aditi, Survey paper on Hilbert transform with its application in signal processing, *Int. J. Comput. Sci. Inf. Technol.* 5 (3) (2014) 3880–3882.
- [45] S. Amandeep, S. Charanjit, Performance Analysis of Cyclostationary spectrum sensing over different fading channels, *Int. J. Comput. Appl.* 129 (1) (2015) 27–31.
- [46] B. Pankaj, Saloni, Spectrum Sensing in Cognitive Radio by Statistical Matched Wavelet Method and Matched Filter, *International Journal of Electronics & Communication Technology* 7 (1) (2016) 33–39.
- [47] *Continuous Wavelet Transform (Advanced Signal Processing Toolkit)*, Online, Available at https://zone.ni.com/reference/en-XX/help/371419D-01/lvasptconcepts/wa_cwt/, (2017) Accessed 17/08/2017.
- [48] H. Arslan, Y. Tevfik, A survey of spectrum sensing algorithms for cognitive radio applications, *IEEE Commun. Surv. Tutorials* 11 (1) (2009) 116–130.
- [49] G. Manikandan, N. Mathavan, M. Suresh, M. Paramisivan, V. Lavanya, Cognitive radio spectrum sensing techniques – a survey, *Int. J. Adv. Eng. Technol.* VII (II) (2016) 48–52.
- [50] M. Rajkumari, E. Varadharajan, Discrete wavelet transform based spectrum sensing in cognitive radios using eigen filter, *Int. J. Adv. Eng. Technol.* 3 (1) (2012) 1–3.
- [51] K. Singh, S.B. Avtar, Study of spectrum sensing techniques in cognitive radio: a survey, *Int. J. Soft Comput. Eng.* 5 (3) (2015) 97–100.
- [52] M. Niranjana, K. Rajashri, Cognitive radio spectrum sensing: a survey, *International Conference on Electrical, Electronics, and Optimization Techniques*, 2016, pp. 3233–3237.
- [53] G. Priya, M. Megha, Analysis of different spectrum sensing techniques in cognitive radio network, *Int. Res. J. Eng. Technol.* 2 (5) (2015) 573–577.
- [54] Z. Yonghong, L. Ying-Chang, Eigenvalue based spectrum sensing algorithms for cognitive radio, *IEEE Personal, Indoor, and Mobile Radio Communications Conference*, 2009, pp. 1–11.
- [55] L. Yuan, M. Lu, A wideband spectrum sensing method based on compressed sensing by using matching pursuits, *Comput. Sci. Eng.* 5 (1A) (2015) 15–22.